SINTEF
PROCEEDINGS
2

Proceedings of the 12th International Conference on Computational Fluid Dynamics in the Oil & Gas, Metallurgical and Process Industries

Progress in Applied CFD – CFD2017

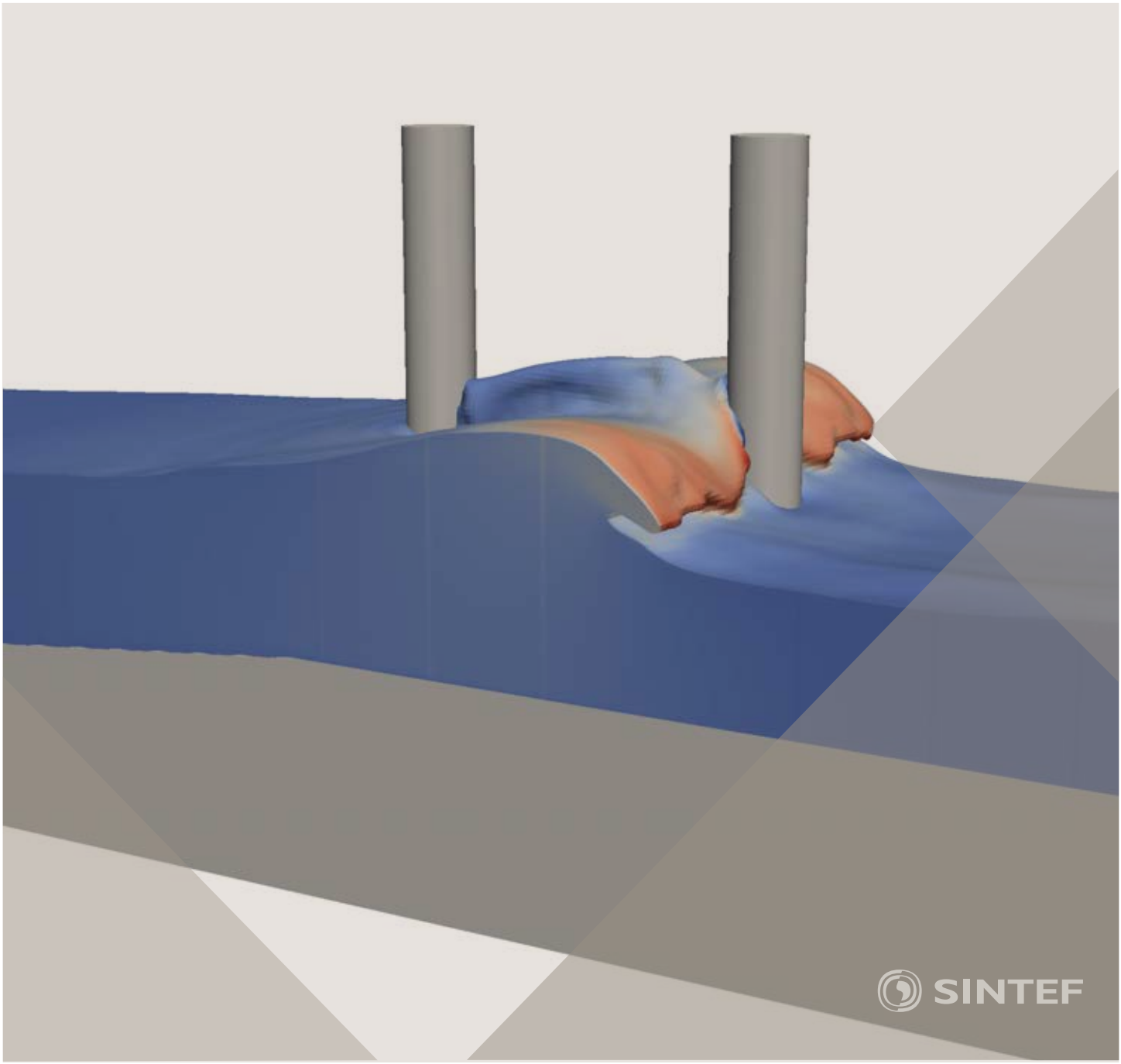

SINTEF Proceedings

Editors:
Jan Erik Olsen and Stein Tore Johansen

Progress in Applied CFD – CFD2017

Proceedings of the 12th International Conference on Computational Fluid Dynamics in the Oil & Gas, Metallurgical and Process Industries

SINTEF Academic Press

SINTEF Proceedings no 2
Editors: Jan Erik Olsen and Stein Tore Johansen
Progress in Applied CFD – CFD2017
Selected papers from 10th International Conference on Computational Fluid Dynamics in the Oil & Gas, Metallurgical and Process Industries

Key words:
CFD, Flow, Modelling

Cover, illustration: Arun Kamath

ISSN 2387-4295 (online)
ISBN 978-82-536-1544-8 (pdf)

SINTEF Academic Press
Address: Forskningsveien 3 B
PO Box 124 Blindern
N-0314 OSLO
Tel: +47 73 59 30 00
Fax: +47 22 96 55 08

www.sintef.no/byggforsk
www.sintefbok.no

SINTEF Proceedings
SINTEF Proceedings is a serial publication for peer-reviewed conference proceedings on a variety of scientific topics.
The processes of peer-reviewing of papers published in SINTEF Proceedings are administered by the conference organizers and proceedings editors. Detailed procedures will vary according to custom and practice in each scientific community.

PREFACE

This book contains all manuscripts approved by the reviewers and the organizing committee of the 12th International Conference on Computational Fluid Dynamics in the Oil & Gas, Metallurgical and Process Industries. The conference was hosted by SINTEF in Trondheim in May/June 2017 and is also known as CFD2017 for short. The conference series was initiated by CSIRO and Phil Schwarz in 1997. So far the conference has been alternating between CSIRO in Melbourne and SINTEF in Trondheim. The conferences focuses on the application of CFD in the oil and gas industries, metal production, mineral processing, power generation, chemicals and other process industries. In addition pragmatic modelling concepts and bio-mechanical applications have become an important part of the conference. The papers in this book demonstrate the current progress in applied CFD.

The conference papers undergo a review process involving two experts. Only papers accepted by the reviewers are included in the proceedings. 108 contributions were presented at the conference together with six keynote presentations. A majority of these contributions are presented by their manuscript in this collection (a few were granted to present without an accompanying manuscript).

The organizing committee would like to thank everyone who has helped with review of manuscripts, all those who helped to promote the conference and all authors who have submitted scientific contributions. We are also grateful for the support from the conference sponsors: ANSYS, SFI Metal Production and NanoSim.

Stein Tore Johansen & Jan Erik Olsen

Organizing committee:

Conference chairman: Prof. Stein Tore Johansen
Conference coordinator: Dr. Jan Erik Olsen
Dr. Bernhard Müller
Dr.Sigrid Karstad Dahl
Dr.Shahriar Amini
Dr.Ernst Meese
Dr.Josip Zoric
Dr.Jannike Solsvik
Dr.Peter Witt

Scientific committee:

Stein Tore Johansen, SINTEF/NTNU
Bernhard Müller, NTNU
Phil Schwarz, CSIRO
Akio Tomiyama, Kobe University
Hans Kuipers, Eindhoven University of Technology
Jinghai Li, Chinese Academy of Science
Markus Braun, Ansys
Simon Lo, CD-adapco
Patrick Segers, Universiteit Gent
Jiyuan Tu, RMIT
Jos Derksen, University of Aberdeen
Dmitry Eskin, Schlumberger-Doll Research
Pär Jönsson, KTH
Stefan Pirker, Johannes Kepler University
Josip Zoric, SINTEF

CONTENTS

A MULTI-DOMAIN 1D PARTICLE-REACTOR MODEL FOR PACKED BED REACTOR APPLICATIONS

Mandar TABIB, Schalk CLOETE, John MORUD, Magne LYSBERG, Shahriar AMINI

SINTEF, Trondheim, NORWAY

* E-mail: mandar.tabib@sintef.no,shahriar.amini@sintef.no,john.morud.sintef.no

ABSTRACT

A validated multi-domain 1D particle-reactor model has been developed to simulate packed bed reactor operation. Two main components of the model are: (1) a particle model for simulating the radial distribution of chemical species and temperature within the catalyst particles and (2) a 1D reactor model for solving mass and energy transport along the length of the reactor. The model captures the effect of intra-particle heat and mass transfer phenomena on the reactor performance. Its efficacy and usability is evaluated using a thorough verification and validation campaign. Validation has been carried out through comparisons to analytical solutions for: (a) the transient thermal response of the fixed bed to a step-change in inlet feed temperature and for (b) the maximum temperature rise during an exothermic oxidation process in a chemical looping combustion (CLC) operation. Further, its performance has been verified with two well-established solvers (a 1D Euler-Euler packed bed model developed in ANSYS FLUENT and a previously published 1D model) for simulating a realistic 500kW cyclic packed bed chemical looping combustion system involving dynamic fuel-air cycling. This successful verification demonstrates the ability of the model to simulate complex cyclic packed bed reactor processes involving stiff kinetics in an efficient manner. Further, significance of particle model is evaluated for mass transfer limiting condition and this reinforces the advantage of using the proposed 1D particle-reactor model in such cases.

Keywords: 1D model, packed bed reactor, chemical looping combustion.

NOMENCLATURE

Ck	Concentration species "k"	[kmol/m^3]
Cp	Heat capacity	[J/kg.K]
Ctot	Total gas concentration	[kmol/m^3]
$D_{eff,kg}$	Effective diffusivity of gas species 'k'	[m^2/s]
$D_{eff,ks}$	Effective diffusivity of gas species 'k' in the pores of the particle.	[m^2/s]
dp	Particle diameter	[m]
Fh	Flux of enthalpy	[J/m^2.s]
Fk	Flux of species "k"	[kmol/m^2.s]
Ftot	Total gas flow rate	[kmol/m^2.s]
G	Mass flux of gas	[kg/m^2.s]
H	Enthalpy	[J]
hc	Heat transfer coefficient	[W/m^2.K]
$\vec{J}$	Diffusive flux	[kg/m^{2}s]
K_{sg}	Interphase momentum exchange coefficient	[kg/m^{3}s]
kg	Mass transfer coefficient	[m/s]
M	Molecular Weight	[Kg/kmol]
Nu	Nusselt number	
p,P	Pressure	[bar]
R	Particle radius	[m]
Rg	Gas constant	[J/kmol.K]
R^H	Het. reaction rate	(kmol/m^{3}s)
S	Source term	
T	Temperature	[K]
T0	Initial temperature	[K]
U	Internal energy	[J/m^3]
Xj	Conversion of species j during reaction	[-]
vg	Superficial gas velocity	[m/s]
wf	Fluid mass flow rate	[Kg/s]
wact,j	weight fraction of active solid species j in pellet.	[-]
wg,i	Weight fraction of gas species i	[-]
Z	Axial position	[m]
c_∞	Concentration at infinity	[any consistent]

Greek Symbols

α	Volume fraction	
γ	Stoichiometric coefficient	[-]
H_{sg}	Interphase energy exchange coefficient	[-]
$\bar{\bar{\tau}}$	Stress tensor	
$\vec{\upsilon}$	Velocity vector	[m/s]
$-\Delta H_{rx}$	Heat of reaction	[J/kmol]
ε	Void fraction	[-]
ε_s	Pore fraction is Oxygen carrier	[-]
η	Reaction efficiency factor	[-]
ξ	Ratio of moles of gas to solid needed for the oxidation reaction	
Γ_k	Source term for species "k"	[kmol/m^3.s]
Γ_u	Source term for enthalpy	[J/m^3.s]
λ	Thermal conductivity in particles	[W/m.K]
λ_{ax}	Effective axial thermal conductivity in bed	[W/m.K]
μ	Gas viscosity	[kg/m.s]
ρ	Gas density	[kg/m^3]
ρ_s	Oxygen carrier density	[kg/m^3]
τ	Oxygen carrier tortuosity	[-]
β	Ratio of thermal capacity of solid and gas.	[-]

Latin Symbols

a	Characteristic length, [m].
p	Pressure, [Pa].
u	Velocity, [m/s].

Sub/superscripts

p or s	Particle/Solid
g or gas	Gas phase
k	Species "k"
l	Reaction "l"

INTRODUCTION

Packed bed reactors are commonly utilized in processes involving solid-catalysed reactions and/or heterogeneous gas-solid reactions [1, 2]. These reactors are used ubiquitously in the petroleum and petrochemical industry for processes involving reforming, hydro-cracking, polymerization, etc. Recently, gas-solid processes have been developed for reducing greenhouse gas emissions. For example, the Packed Bed Chemical Looping Combustion (PBCLC) process has enjoyed significant research attention as a potential solution for cost effective power production with integrated CO2 capture [3, 4].

A validated stand-alone packed bed reactor simulator will help to ensure a safe and efficient packed bed reactor operation. Hence, a computationally efficient 1D particle-reactor model has been developed to accurately capture the physics. The concept of multi-domain 1D particle-reactor models have been used effectively by different researchers [5-9]. Different researchers have used different set of equations and solution techniques in their models. However, in most cases, the models have been applied on a single stage operation rather than on cyclic operations. In present work, the equations and solvers/solution techniques used are different than those proposed in earlier models. The usability and efficiency of the proposed model is evaluated by verifying it with other popular well-established solvers, like ANSYS FLUENT and a published 1D model from the Eindhoven University of Technology [3, 7, 8]. The verification is done for a realistic cyclic packed bed chemical looping combustion (PBCLC) process operation. The cyclic reduction-oxidation process involves very stiff kinetics and is useful to test the robustness and accuracy of our software. Further, validation of the proposed model has also been presented by comparing it with analytical solutions for: (a) the transient thermal response of the fixed bed to a step-change in inlet feed temperature and for (b) the maximum temperature rise during an exothermic oxidation process in a chemical looping combustion (CLC) operation.

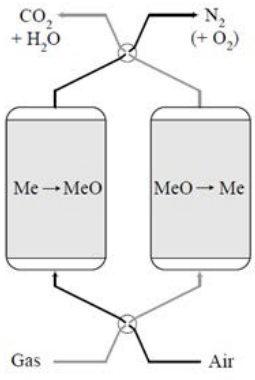

Figure 1: Chemical Looping Combustion process in a packed bed reactor.

The PBCLC process involves cyclic gas-solid non-catalytic reaction operations, wherein the bed material (typically a metal oxide oxygen carrier) is alternatively exposed to a fuel stream (reduction cycle) and an air stream (oxidation cycle). Figure 1 shows a schematic representation of a PBCLC reactor system. During the fuel stage, the oxygen carrier supplies oxygen to the fuel, resulting in a hot stream of carbon dioxide and super-heated steam which can subsequently be processed into a high-purity CO2 stream following heat recovery and purification. The reduced metal oxide bed is then exposed to the air stream, which re-oxidizes it. This highly exothermic oxidation stage produces a high-volume stream of hot gas that can also be used for efficient electricity generation in a combined cycle. The reduction-oxidation cycle is then repeated continuously, leading to power generation with integrated CO2 capture. The 1D particle-reactor model can help to determine the operating conditions (flow rates, flow composition and feed inlet temperatures) and reactor size for efficient PBCLC operation.

MODEL DESCRIPTION

A 1D model assuming plug flow conditions can be safely applied to industrial scale packed bed reactors because the effect of near wall phenomena in packed beds (oscillations in radial volume fraction profile) is confined to a very small zone (typically about 5 particle diameters from the wall). Radial variations in volume fraction and velocity are negligible beyond this small near-wall zone. In addition to the plug-flow assumption, the present 1D model also considers the process to be adiabatic and the ideal gas law is considered to be valid. The model accounts for (a) external heat and mass transfer resistances, which influence the transport of reactants and energy from bulk fluid up to a catalyst pellet, (b) intra-particle transport (diffusion limited) resistances, which influence the transport of mass and energy from the external surface of the particle to grains inside the porous pellet, and (c) the kinetic rate, which accounts for the reactions occurring on internal grains as the fluid phase reactant reaches it. These physical phenomena are captured by solving species mass balance and energy balance equations for the fluid phase and the reaction-diffusion equations within the particle. The particle model provides the source-term for the mass and energy balances of the fluid phase by computing the component and energy fluxes at the particle surface. Thus, the particle model and reactor model are coupled together by the source terms. The equation system is described in more detail below.

Gas phase Equations

Ideal gas equation of state

$$P = C_{tot} R_g T_g \quad (1)$$

Ergun pressure drop equation

$$\frac{\partial P}{\partial z} = -\frac{G}{\rho d_p}\left(\frac{1-\varepsilon}{\varepsilon^3}\right)\left(\frac{150(1-\varepsilon)\mu}{d_p} + 1.75\ G\right) \quad (2)$$

Material balance for species "k" in gas phase

$$\varepsilon \frac{\partial C_k}{\partial t} + \frac{\partial F_k}{\partial z} = \Gamma_k$$

$$where,\ F_k = F_{tot} X_k - C_{tot} D_{eff,kg} \frac{\partial X_k}{\partial z} \quad (3)$$

Energy balance for gas phase

$$\varepsilon \frac{\partial U}{\partial t} + \frac{\partial F_h}{\partial z} = \Gamma_U$$

$$where,\ F_h = F_{tot} h - \lambda_{ax} \frac{\partial T}{\partial z} \quad (4)$$

Boundary conditions for gas phase

z=0: Inlet flux

z=L:

$$\frac{\partial C_k}{\partial z} = 0,\ \frac{\partial T}{\partial z} = 0 \quad (5)$$

Source terms for gas phase mass- and energy balance arising due to mass and heat transfer at the gas-particle interface.

$$\Gamma_k = k_g a\left(C^s_{k,r=R} - C_k\right) \quad (6)$$

$$\Gamma_U = h_c a(T^s_{r=R} - T) \quad (7)$$

Where, hc is the heat transfer coefficient and kg is the mass transfer coefficient.

Solid particle model (particle could be oxygen carrier or catalyst)

Mass balance for species "k" inside catalyst particles

$$\varepsilon_s \frac{\partial C^s_k}{\partial t} = \frac{\varepsilon_s D_{eff,ks}}{\tau} \nabla^2 C^s_k + \rho_s r_k \quad (8)$$

Energy balance for catalyst particles

$$\rho_s C_{ps} \frac{\partial T^s}{\partial t} = \lambda \nabla^2 T^s + \rho_s \sum_l r_l \left(-\Delta H_{rx,l}\right) \quad (9)$$

Boundary conditions for catalyst particles

Symmetry at r=0:

$$\frac{\partial C^s_k}{\partial r} = 0\ ,\frac{\partial T^s}{\partial r} = 0 \quad (10)$$

Catalyst surface, r=R:

$$-\frac{\varepsilon_s D_{eff,ks}}{\tau} \frac{\partial C^s_k}{\partial r} = k_g \left(C^s_{k,r=R} - C_k\right) \quad (11)$$

$$-\lambda \frac{\partial T^s}{\partial r} = h(T^s - T) \quad (12)$$

Numerical solution of this equation system results in temperature and composition profiles along the length of the bed for both the gas and solid particle. The velocity of the solid particle is set to zero. The pressure at any given cell is obtained by ideal gas law (Equation 1) and pressure drop between this cell and the outlet is obtained. This pressure drop is used to compute the gas phase velocity using a pressure drop correlation (Equation 2). The pressure drop correlation accounts for the resistance offered by the particles to the gas flowing through the interstitial region. The closures used by the 1D model are dependent on particle shape and size. A spherical particle of size 3 mm is used in this work. For spherical particles, the following well-established correlations have been used : (a) the pressure drop correlation by Ergun [10] as in Equation 2, (b) the heat transfer correlation using the multi-particle Ranz-Marshal correlation [11] for computing external heat transfer coefficient and (c) the mass transfer correlation for computing mass transfer coefficient. Further, information on (a) the volume fraction of the gas phase and (b) the particle surface area per unit volume of the reactor, are also needed as closures by the model. For packed beds comprising of spherical particles, the solid volume fraction in the bed (around 0.6) and surface area of particle per unit volume of reactor, a, are known. Thus, well-known closures and correlations for the spherical particle are used in this study. For many non-spherical particle shapes, however, these critical closure values are not known. One way of obtaining them is using a 3D CFD-DEM modelling approach such as developed by Tabib [12].

NUMERICAL IMPLEMENTATION AND SOLVER DETAILS

The set of partial differential equations (Equations 3-12) are solved using Finite Volume discretization for the gas phase in the reactor (where the bed is spatially divided into small volumes in the axial direction) and an orthogonal collocation technique for the particle. The orthogonal collocation technique resolves the radial variations of temperature and chemical composition within the particle at each axial location of the bed. Figure 2 shows the schematic representation of this implementation. The mass and energy balances are formulated for gas and particle phases and solved for each cell volume.

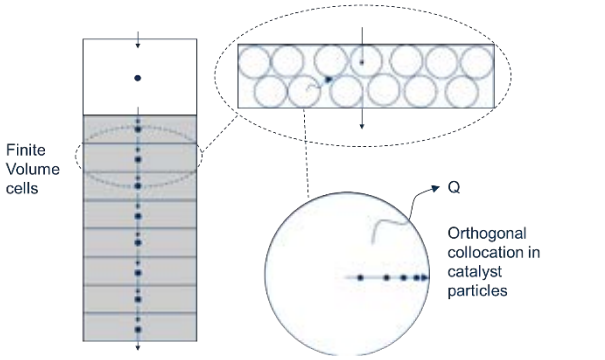

Figure 2: Implementation of 1D Particle-Reactor Model.

The partial differential equations are converted into a set of ordinary differential equations (ODE) by discretizing the spatial terms of the gas phase equation. An upwind scheme is used to obtain the flux at cell faces for computing the convective term in the discretized equation. The resulting ODE equation set can be solved by using any available standard ode-solver that can solve for stiff equations. An ODE solver proposed by Hindmarsh's group [13-15] has been used in this work. The temporal discretization is done using an implicit multi-step backward differentiation formula and the Adam-Moulton scheme. This implicit temporal discretization forms a non-linear algebraic equation system that needs to be solved at each time-step. A Newton scheme is used to solve these non-linear equations iteratively.

The Newton scheme uses a Jacobian matrix of the system of equations. This Jacobian matrix can be a banded matrix or a full matrix depending upon the way

equations are arranged and solved. A banded Jacobian matrix implementation ensures faster and more efficient solution. The equations to be solved (Equations 3-12) are arranged in a manner so as to produce a banded Jacobian matrix. Here, the equations (variables) to be solved are arranged cell-wise, i.e., equations in the first cell volume are arranged first (all gas species mass balance equations in the first cell, all solids species mass balance equations in the first cell, one gas energy equation in the first cell, one solid energy equation at first cell), followed by the same variables in the second cell volume, then the third cell volume and so on. This produces a banded Jacobian pattern. If we arrange the equations in a different way and not cell-wise (such that equations of a particular variable for all N cells are solved first), then it leads to an inefficient solution involving the full Jacobian matrix. Hence, a banded Jacobian solver implementation is executed.

MODEL VALIDATION

Packed beds are characterized by the presence of either or both a thermal front and the reaction front. The thermal dynamics of the bed and movement of the thermal front influences many processes, like catalytic chemical reactors, adsorption columns, ion exchange columns, and the chromatographic process. In heterogeneous gas-solid reactions (e.g., chemical looping combustion), the reaction front is also present along with the thermal front. Both these fronts are identifiable via the temperature and concentration profiles along the bed.

The reaction front velocity is determined by the reactant species concentration in gas and solid phase, the molecular weights of reacting species, and the stoichiometry of the reaction rate. An identifiable feature of this reaction front is the presence of a fully converted solid bed upstream of the front (i.e., no solid reactant species exist and no reaction takes place upstream of the reaction front), while the solid bed region that is downstream of the reaction front will be fully unconverted and will react on being exposed to a gaseous reactant. Depending upon the rate of the reaction, the reaction front can be diffused or sharp. A rise in temperature of gas and solid bed occurs owing to the heat generated at the reaction front. The reaction front can also be identified by temperature profiles as there will be a drop in bed-temperature just downstream of the reaction front (if the reaction is exothermic). On upstream regions of the reaction front, hot temperatures will prevail till certain distance until the bed is cooled down by incoming gas. This temperature difference between the incoming cold gas and the hot converted solid bed leads to heat transfer and establishment of a thermal front. Velocity of this thermal front is determined by relative thermal heat capacity of the fluid and the bed (depends upon material properties like heat capacity and density). The above description assumes that reaction front velocity is faster than thermal front velocity. A 1D model should be able to accurately capture the movement of these two fronts (thermal and reaction fronts). Hence, validation of the 1D model is done by comparing it with analytical results for the movement of the fronts and the maximum temperature rise experienced in the reaction front. The validation for the two cases is discussed below.

VALIDATION

Case - Transient thermal response of the bed involving a step change in feed temperature

The 1D model is used to simulate the transient temperature response in the bed for a step increase in the inlet feed stream temperature and no reactions are considered. There exists an analytical solution [16] for this case if the following idealizations are considered: (a) negligible thermal capacity of the reactor walls, (b) negligible radial or azimuthal temperature gradients in the fluid and solid phases, (c) plug flow is assumed, (d) negligible axial mixing of fluid due to dispersion, (e) negligible axial conduction of heat in either fluid or solid media and (f) negligible temperature gradients within the solid particles. The equations (equation 13-14) to be solved analytically can then be represented by the following heat balances on both the fluid and solid.

Heat balance in fluid medium

$$\rho_g C_{p,g} \varepsilon A \frac{\partial Tg}{\partial t} + wC_f \frac{\partial Tg}{\partial x} = haA(T_s - T_g) \quad (13)$$

Heat balance in solid medium

$$\rho_s C_s (1-\varepsilon) A \frac{\partial Ts}{\partial t} = haA(T_g - T_s) \quad (14)$$

Initial condition: Both solid and fluid at same uniform temperature, T0.

Boundary condition: A step change in fluid temperature at the bed inlet.

$$T(0,t) = T_0 + \alpha T \quad (15)$$

The dependent variables above (temperature) can be normalized using a step change in temperature, and independent variables (time and spatial location) can be normalized by dividing it with fluid residence time and reactor length respectively. The new equations in terms of normalized variables can be written as:

$$\frac{\partial \theta}{\partial \tau} + \frac{\partial \theta}{\partial z} = H(\phi - \theta) \quad 16$$

$$\frac{\partial \emptyset}{\partial \tau} = H\beta(\theta - \phi) \quad 17$$

IC $\theta(z,0) = \phi(z,0) = 0$

BC $\theta(0,\tau) = U(\tau)$

where, $\tau = \frac{tv}{L}$, $z = \frac{x}{L}$, $\phi = \frac{T_s - T_0}{\alpha}$, $\theta = \frac{T - T_0}{\alpha}$, $H = \frac{haL}{\rho_f C_f \varepsilon v}$, $\beta = \frac{\rho_f C_f \varepsilon}{(1-\varepsilon)\rho_s C_s}$

The "average response time" is dependent on the number of fluid transits , H (fluid residence time) needed to supply the thermal capacity of the bed, which is determined by β (ratio of heat capacitance).

Equations 16-17 are solved analytically by subjecting them to Laplace transform and substituting for the particle temperature in the fluid energy balance, which leads to the equation 18 below.

$$\theta(s,z) = \frac{1}{s} exp\left[-sz - \frac{Hsz}{s+H\beta}\right] \quad 18$$

Inverse Laplace transform of above equation can provide us with the solution for fluid temperature at any location (z) at any time (t) as shown in Figure 3 for the case below.

Case Studied

Consider a packed bed reactor with an inlet gas fed at a temperature equal to the initial temperature of the bed (say, at 571 K). A step change in feed

temperature is provided and inlet gas temperature is increased to 623 K (a step change of 52 K). The transient response of bed is studied for fixed material properties of the gas and solids phases (fixed heat capacity ratio, β of 2 x 10-4) for three different cases. The three cases have been studied by varying the external heat transfer coefficient between gas and solid (at h = 6 W/m^{2}K, 60 W/m^{2}K and 600 W/m^{2}K).

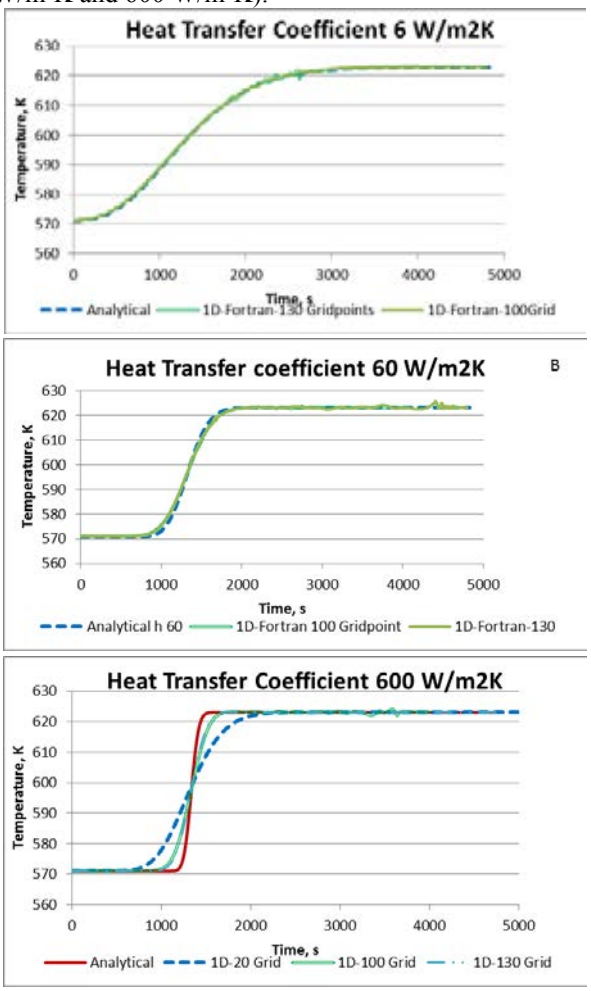

Figure 3: Validation of transient thermal bed response.

The 1D model has been compared to the analytical solution for these three different cases (Figure 3A-C) using three different grid sizes (20, 100 and 130 grid points). Grid-independence has been achieved with 100 grid points. The velocity of the thermal front and the average response time for the effect of inlet step change to be felt at any particular location is dependent on the ratio of thermal capacities of gas and solid (β). The three figures show that for the chosen value of $\beta = 2 \times 10^{-4}$, the average response time for the effect of inlet step change to be felt at reactor bed outlet is 1334 s.

The rate of fluid-particle heat transfer (or heat transfer coefficient) has no influence on the average response time, but determines the sharpness of the temperature profile. A very high heat transfer coefficient value results in faster gas-solid heat transfer and low (or negligible) dispersion in the temperature profile around the average response time (i.e. the outlet temperature profile will then resemble the inlet step change profile), while a lower heat transfer coefficient will result in highly diffused response to the step change. This effect can be seen in Figure 3(A-C).

The 1D model correctly captures the more diffused heat front at heat transfer coefficient of 6 W/m^{2}K and 60 W/m^{2}K, but the solution for the high heat transfer coefficient (600 W/m^{2}K) could not be fully replicated. This sharp step change response can be captured by using very high number of grid points and significant numerical diffusion is still observed for the finest grid investigated (130 grid points). A higher order scheme (like, central difference) may perhaps show lower dispersion than an upwind scheme, but it may also introduce spurious oscillations and is known to be unstable for flows with Peclet number greater than 2 [17]. However, typically the gas-solid heat transfer coefficient in a packed bed will not be as high as 600 W/m^{2}K and the cyclic CLC process studied here has a heat transfer coefficient of 100 W/m^{2}K. Thus, it can be concluded that the present 1D model is able to capture the thermal front movement for moderate heat transfer coefficients which are typical of packed beds.

Case - Validation of Temperature Rise During An Exothermic Reaction

In order to validate reactive behaviour, the 1D model is used to simulate the movement of the reaction and thermal fronts during the oxidation stage of a PBCLC process. The movement of fronts and the maximum temperature rise predicted by the 1D model is compared to that predicted by an analytical model [3]. There exists an analytical solution if the following conditions are assumed: (a) the rate of non- catalytic gas–solid reaction is infinite, (b) axial conduction and dispersion effects are negligible, (c) heat and mass transfer limitations between the gas and solid phase are negligible and (d) intra-particle diffusion limitations are negligible. The case considered initially has the solid bed (the oxygen carrier) made of ilmenite (FeO-Fe2O3-TiO2) in a fully reduced state (i.e. no Fe2O3, but only FeO-TiO2). The solid particle has a density of 2591 kg/m3, a heat capacity of 922 J/KgK and an active FeO weight fraction of 0.21. The initial gas present in the bed (nitrogen) is non-reactive. Both phases are initialized at a uniform temperature of 923 K. The system is fed with air at inlet temperature of 923 K and atmospheric pressure (density varies as per ideal gas law). As the oxygen is exposed to the solid limonite particle, the exothermic oxidation reaction (4FeO + O2 → 2Fe2O3) takes place and proceeds to completion. The resulting reaction front propagates through the bed at a velocity shown by Equation 24. The expression for computing reaction front velocity assumes that all the gaseous reactant reacts with a known stoichiometric amount of the solid material.

$$w_r = \frac{\rho_g w_{g,i}^{in} v_g M_{act,i}}{\varepsilon_s \rho_s w_{act,j} X_j M_i \xi} \qquad 24$$

The reaction front velocity obtained for the present case (as per equation 24) is 7.67 x 10^{-2} m/s, allowing the distance travelled in 15 s of oxidation to be calculated as 1.15 m. Figure 4 shows the results obtained by the 1D model simulation for five different grid sizes (20, 40, 60, 80 and 100 grid points) and one result is shown by making transport resistances negligible (i.e., employing very high values for mass diffusivity). The grid-independent results show a dispersed (diffused) reaction

front and the mid-point of this dispersed reaction front is at 1.15 m from the inlet of reaction bed. The reaction front dispersal is along the expected lines as the overall reaction rate is not infinite as is assumed in equation 24. Figure 4 also shows that particle-scale mass transfer resistances (captured by the particle model) cause the fronts to become more diffused. Thus, it can be concluded that the 1D model correctly captures the movement of the reaction front.

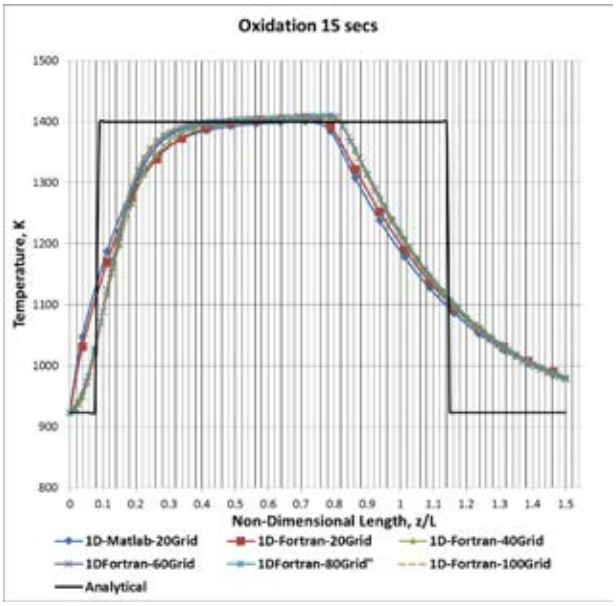

Figure 4: Validation of 1D model for front movement and temperature rise for an exothermic reaction : Analytical model (solid black line) compared with results from 1D-model at five different grid points (20,40,60,80,100) and from 1D model with no diffusional limitation (at 100 grid points).

The heat released during the exothermic reaction le: $_A$ to the establishment of a higher maximum temperature upstream of the reaction front (which is discussed in a later section). Bed material upstream of the reaction front will remain hot for some distance until it is cooled down by incoming gas. The incoming gas (at 923 K) on getting exposed to a hot and fully converted bed, will therefore establish a thermal front as described in the previous section.

The thermal front moves at a velocity w_h as expressed by equation 25. This expression assumes that at the heat front, the heat present in the solid material is instantaneously transferred to the gas phase.

$$w_h = \frac{\rho_g v_g C_{p,g}}{\varepsilon_s \rho_s C_{p,s}} \qquad 25$$

The thermal front velocity predicted by the above equation for the current case is 5.76 x 10^{-3} m/s (around one order of magnitude slower than the reaction front). In 15 s of oxidation, the thermal front would travel 0.086 m inside the reactor bed. Figure 4 obtained by the 1D model shows the thermal front to be dispersed around 0.086 m from inlet of the bed due to the finite heat transfer coefficient. The model thus predicts the movement of the thermal-front reasonably well.

The maximum temperature that can be reached in the bed due to the heat of reaction can be obtained using an energy balance. The energy balance formulation assumes that the volumetric heat capacity of the gas phase can be neglected and that the reaction front propagates more rapidly than the heat front. The energy balance equation can be written as:

$$\frac{\rho_g v_g w_{g,i}^{in}}{M_{g,i}}\left(-\Delta H_{R,i}\right) = \varepsilon_s \rho_s C_{p,s}(w_r - w_h)(T - T_0) \qquad 26$$

Equations (24)–(26) can then be combined to obtain the expected temperature change (as shown in equation 27).

$$\Delta T = \frac{\left(-\Delta H_{R,i}\right)}{\frac{C_{p,s} M_{a,i}}{w_{act,j} X_j \tau} - c\frac{C_{p,g} M_i}{w_{g,i}^{in}}} \qquad 27$$

Equation 27 shows that the maximum temperature in the reactor is independent of the process inlet gas flow rate and is dependent upon the heat of reaction, material properties, stoichiometry and reactant species composition in gas inlet and initial solid bed. The maximum temperature change predicted by equation 27 is about 477 K which is correctly reproduced by the model as shown in Figure 4. Thus, the 1D model is able to capture the movement of the thermal and reaction fronts as well as the maximum temperature rise. This validates the use of 1D model for heterogeneous gas-solid reactions such as those taking place in the PBCLC process.

VERIFICATION

The 1D particle–reactor model has been verified by comparing its performance with a 1D Euler-Euler model developed in ANSYS FLUENT and with a well-established 1D model developed at the Eindhoven University of Technology (TU/e). The ANSYS FLUENT solver is recognized for being robust, computationally efficient (high convergence speed) and numerically stable (use of large time-steps). It is widely used and has been extensively validated for reactive multi-phase applications. The TU/e model has been used in a number of publications [7, 8, 18] implying that its validity is broadly accepted within the scientific community. These two simulation tools therefore present an excellent verification benchmark.

The verification has been done for realistic cyclic operating conditions suggested for the 500 kW demonstration scale CLC reactor [18]. The simulation with these operating process conditions (see B1 strategy from Table 4 of [18]) will help to evaluate the model for real behaviour of an industrial packed bed reactor. This operating cycle strategy includes four distinct phases of operation: a reduction phase (with synthesis gas as fuel) for 300 s, a heat removal phase with an inert gas stream for 300 s, an oxidation phase with air (until the oxidation reaction front reaches the end of the reactor) for 300 s, and a purge phase for 10s. This 910 s cycle of reduction-heat removal-oxidation-purge is repeated continuously. The advantage of this approach is that the reduction phase is carried out when almost the entire bed is at the maximum temperature (owing to a prior oxidation phase). At lower temperatures, the reduction reaction rates are quite low. Hence, a bed at maximum temperature enables a higher reduction reaction rate and avoids early fuel-slip of H2 and CO.

The proposed model must be able to capture the effect of a typical cyclic operation, wherein the initial bed conditions (bed temperature and species) for a newly starting phase is a result of a previous phase in the cycle. These process conditions therefore serve as a very stringent test of the model's ability to accurately capture the thermal and chemical dynamics of packed bed reactors.

The reduction and oxidation reactions taking place for the ilmenite particle can be described as :

$$H_2 + Fe_2O_3 \rightarrow 2FeO + H_2O$$

$$CO + Fe_2O_3 \rightarrow 2FeO + CO_2$$

$$O_2 + 4FeO \rightarrow 2Fe_2O_3$$

All three models use the same reaction kinetics provided by Abad et. al. (2011). However, the set of equations and modelling approach used by all the three models are different. The FLUENT model does not have a particle model, while the TU/e model has both a particle model and reactor model [7, 8]. However, the TU/e cyclic simulations presented by Spallina et. al. [18] were conducted without the use of a particle model (using an effectiveness factor approach with near unity value of effectiveness factor) for efficient computation. The next section describes the 1D Fluent model in brief.

1D Fluent Model

The 1D FLUENT model uses an Eulerian-Eulerian multiphase flow modelling approach, where the two participating phases (gas and solids) are treated as inter-penetrating continua or fluids. The mass, momentum, energy and species are conserved for each phase individually. Table 1 lists the conservation equations being solved by the FLUENT solver and the closure laws (Ergun drag model and multi-particle Ranz-Marshall heat transfer coefficient) used. For maintaining the packed bed, the solid phase velocity is fixed to zero and the volume fraction of both solid and gas phase are also fixed.

The reactor geometry comprises of a plane (0.3 m x 2.8 m), which is spatially discretized only in axial direction (100 grid cells in axial direction) and has no radial space discretization. This enables for only the 1D effect to be solved. Grid independence was achieved for the 100 axial grid point employed. The solutions have been obtained using a phase-coupled SIMPLE algorithm [17] for pressure-velocity coupling. The QUICK scheme [19] has been employed for convective terms discretization in all the equations and a 1st order implicit scheme temporal discretization has been used. The comparison of the three models is as below :

The three models (1D Fluent, 1D TU/e and 1D particle-reactor) have been compared for predicting the axial temperature profile (Figure 5) at the end of oxidation phase, at the end of reduction phase and at the end of heat removal phase in a cyclic operation. In addition, the reduction reaction front movement (Figure 6) and the exit gas temperature in a cycle (Figure 7) are also compared.

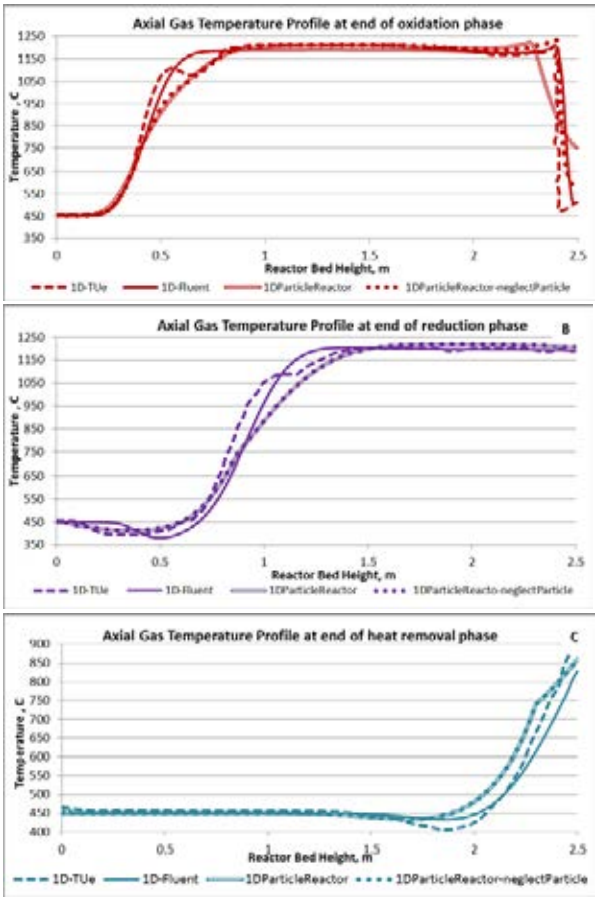

Figure 5 Verification - comparison of different 1D model in predicting the axial temperature profile at: (A) the end of oxidation phase, (B) at the end of reduction phase and (C) at the end of heat removal phase.

Simulations have also been conducted to check the effect of diffusive resistances within the particle on the whole cyclic process. To make the particle effect of negligible, the 1D particle-reactor model has been simulated with high intra-particle gas species diffusivity and high external heat/mass transfer coefficients (see the results with legend 1DParticleReactor-neglectParticle in Figures 8-11). The inclusion of the particle model has a significant impact. The oxidation reaction front (towards reactor end in Figure 5A) and reduction reaction front (in Figure 5B) are more diffused with the particle effect on (legend named 1DParticleReactor) than without the particle effect (legend named 1DParticleReactor-neglectParticle). This diffused front is caused by a reduction in the effective reaction rate due to inclusion of intra-pellet mass-transfer limitations with the particle. For this particular case, the diffusional resistance offered by the 3 mm spherical particles is high enough to have an impact on the cyclic reactor performance. For example, Figure 8 shows much earlier fuel slip in the model with intra-particle diffusive resistances activated than in the model without these resistances. Such fuel slip would require a significantly shorter fuel stage, thereby changing the overall cycle dynamic.

This significant effect of intra-particle diffusion is expected because diffusivity of species lowers owing to the reduction in mean free path with increasing pressure, implying that diffusivity is low at the 20 bar operating pressure. The effective diffusivity in the particle after

accounting for the particle void fraction and tortuosity leads to a lower diffusion rate constant (around 1.3 s^{-1}) for the 1.5mm radius particle. The Thiele modulus (diffusion time over reaction time) for the present condition is in the order of 100 due to the higher effective reaction rate constant. This implies that the process is mass transfer dominated and provides the theoretical basis for the observed results (as predicted by the inclusion of the particle model).

Hence, the results with inclusion of the particle model give more dispersed profiles as compared to the 1D Fluent and 1D TU/e model results. The inclusion of the particle model in the 1D model helps to correctly identify the significant amount of fuel slip taking place during the reduction phase as seen in Figure 8, which will lead to more accurate reactor design and cycle-time predictions. However, the 1D particle-reactor model with neglected particle effect (legend named 1DParticleReactor-neglectParticle) gives similar results as the 1D TU/e model and the 1D Fluent model.

The oxidation phase temperature rise and the oxidation thermal front velocity predicted by these three models (in Figure 5A) are also quite similar but for some minor deviations. These minor deviations are acceptable and are caused by some minor differences in the material properties data (heat capacity as a function of temperature) and differences in the means of computation of heat of reaction. The TU/e model computes the heat of reaction using an input correlation of heat of reaction as a function of temperature, while the other two 1D models compute the heat of reaction from the input heat capacity data and standard enthalpy of formation.

These three models also show good agreement on the location of the oxidation reaction front (Figure 5A) and the reduction reaction front (Figure 6). The oxidation reaction front is located towards the reactor end (seen in Figure 5A) as the results are compared at the end of the oxidation phase. In Figure 6, the reduction reaction front is located mid-way of the reactor (as the results are compared after 150 s from start of the 300 s reduction phase). The reaction front movement is independent of the reaction rate, but the slope of the front (sharp or diffused) is dependent upon reaction rate. As mentioned earlier, the results of 1D particle-reactor model with particle effect neglected (legend named 1DParticleReactor-neglectParticle) is closer to the 1D Fluent and 1D TU/e model (sharper reaction front) for both the oxidation and reduction reaction front. This is expected as both the 1D Fluent and 1D TU/e model do not include the effect of intra-particle diffusion. The comparison of thermal fronts predicted by the three models at the end of reduction (Figure 5B) and at the end of heat-removal (Figure 5C) shows some minor deviations within acceptable limit. As suggested earlier, these deviations are a result of uncertainty in exact closure data (heat capacity material properties) used by the TU/e model. The heat capacity data and heat of reaction data for a given material system predicted by different thermodynamic software packages and suggested in different material database handbooks may slightly differ from each other, resulting in this acceptable deviation.

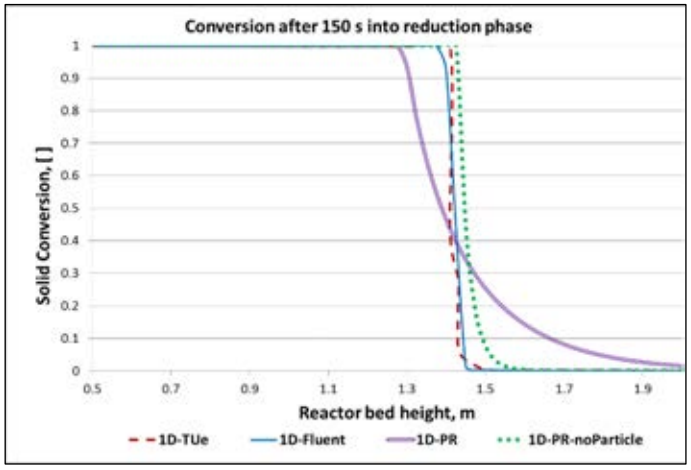

Figure 6 Verification - Comparison of different 1D models in predicting the reaction front velocity during the reduction phase (**PR** in the legend stands for our particle-reactor model).

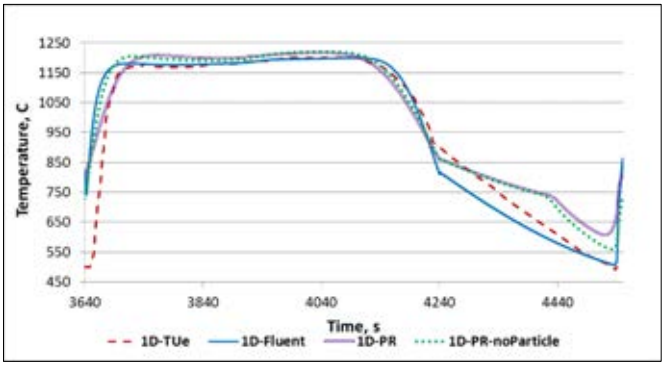

Figure 7 Comparison of different 1D models in predicting the exit gas temperature dynamics in a cycle. (**PR** in the legend stands for our particle-reactor model).

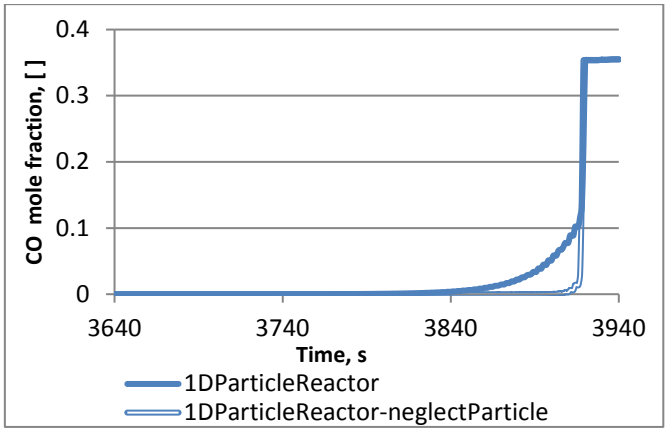

Figure 8. Effect of particle model on Fuel-slip: Outlet concentration of CO mole fraction at reactor exit during the reduction stage.

This uncertainty in material property data also explains the deviation in the last segment of the exit gas temperature profile (Figure 7). However, all three models predict the same maximum outlet temperature (nearly 1200 ºC) for a similar duration of time. Despite the minor deviations caused by uncertainties regarding material property data, the present comparative results on axial temperature profile and solid conversion profile provide

a credible verification of the accuracy of the 1D-particle-reactor model solver developed in this work. The next section covers in brief the performance and advantages of the proposed solver.

Regarding solver efficiency of 1D model, using 100 grid points (for ensuring comparison with grid independent FLUENT results) and using very high tolerances (absolute tolerance of 1 x 10^{-6} and relative tolerance of 1 x 10^{-9}), the 1D particle-reactor model takes 4960 s (about 1.37 hrs) of computational time to simulate 4550 s of cyclic reactor operation. The 4550 s of cyclic reactor operation corresponds to 5 cycles (5 x 910 s = 4550 s). The results after 4 cycles are already compared and discussed in Figure 5-8. Figure 9 shows results from 1D Fluent model. The 1D simulation was run on a desktop personal computer with 2.7GHz Intel® core™ i7-2620M CPU. With 70 grid points, this 1D model gives as accurate results as 100 grid points (nearly grid-independent result), in computational time faster than real-time (i.e. the 4550 s of reactor operation is simulated in 3018 s of computational time). While with 20 grid points, the 4550 s cyclic reactor operation is simulated in just 520 s of computational time, but there is loss of accuracy owing to numerical diffusion (the fronts are more diffused). Comparatively, when the FLUENT solver is run without any convergence criteria, then it is 7 times faster than the 1D model with 100 grid points and ensures real-time operation (simulates 4500 s cycle in just 700 s of computational time). However, the 1D Fluent model does not account for the particle effect. This ANSYS Fluent simulation is carried out on a server machine on a single processor (2.4GHz Intel® Xeon® E-5645 CPU). With convergence criteria on (convergence criteria of 1 x 10^{-3} for all equations), the ANSYS FLUENT 13 solver (with 100 grid points) takes 19 hrs of to simulate the 4550 s cycle. However, the FLUENT solver has been able to capture the front movements in the cycle accurately with little loss of accuracy when run without any convergence control criteria. The segregated solver in conjunction with Algebraic Multigrid method in ANSYS Fluent ensures efficient solution. However, the cost of ANSYS FLUENT licenses along with need for a server infrastructure makes it costly, while the present 1D model provides results as numerically accurate as FLUENT in a very cost-effective way. In addition, the proposed 1D model also simulates for the effect of intra-particle diffusion and makes it physically more complete. Further, the implicit solver utilized makes the model computationally efficient for stiff kinetics. It is not practically feasible to solve the stiff kinetics using explicit schemes as it requires very low time-steps (a fact tested using the explicit ode45 solvers in MATLAB®). The current implicit solver runs with an average time step of 1 x 10^{-3} s for the stiff kinetics as compared to 1 x 10^{-8} s required by the explicit solver. Further, with increasing grid density, an explicit solver performance becomes much slower than the implicit solver. An explicit solver needs to lower the time-step to meet the Courant number criteria for stability, while an implicit solver is not limited by stability but will lower the time-step to meet accuracy (for increasing grid density). The present implicit solver thus ensures faster convergence.

The choice of programming language also ensures faster solutions. The present Fortran-90 implementation makes the code much faster as Fortran-90 is a compiled scripting language. This 1D model implemented in Fortran-90 is two orders of magnitude faster than a similar implicit Matlab® solver (Matlab® being an interpreted scripting language takes longer time).

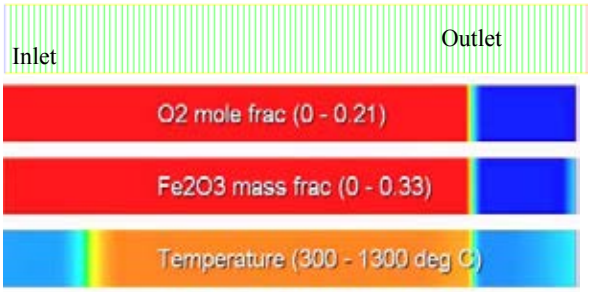

Figure 9 shows the grid and geometry used for 1D Fluent and the location of reaction front and thermal front captured by it during the oxidation phase of the cycle.

Thus, both the validation and verification of the proposed multi-domain 1D particle-reactor model shows that it offers good numerical accuracy, is computationally efficient in solving systems with stiff kinetics, is physically complete as it simulates the particle effect, and is cost-effective for practical operations.

CONCLUSIONS

The 1D multi-domain packed bed model is a combination of (1) a particle model for the radial distribution of chemical species and temperature within a catalyst particle and (2) a 1D reactor model for mass and energy transport along the reactor. The 1D particle-reactor model has been successfully validated against analytical solutions for (a) transient thermal behaviour of a fixed bed to a step-change in inlet feed temperature and for (b) maximum temperature rise and front movement during an exothermic oxidation stage in a packed bed chemical looping combustion process. The 1D model predicts similar results as the analytical models, thus giving confidence in its accuracy and usage. Further, the proposed 1D model is also successfully verified by comparing it with the popular commercial ANSYS FLUENT solver and a well-established 1D packed bed reactor model from the Eindhoven University of Technology. The models are compared for simulating a realistic 500kW cyclic chemical looping combustion process involving stiff redox kinetics over multiple cycles, wherein each cycle comprises of reduction phase, heat-removal phase, oxidation phase and purging phase. These process conditions serve as a very stringent test of the model's ability to accurately capture the thermal and chemical dynamics of packed bed reactors. The comparison reveals that the proposed model is able to accurately capture the thermal front and reaction front dynamics arising in the realistic 500kW cyclic PBCLC process. The proposed 1D model predicts similar results as the 1D FLUENT and 1D TU/E model when the particle effects are made negligible by using high transport coefficients. The comparison also highlights the need and significance of a particle model when the mass transfer limitation dominates, and thus successfully showcases the advantages with using the proposed 1D particle-reactor model. The validated and verified 1D

model is also compared for the solver performance. The choice of an implicit multi-step backward differentiation formula makes the model computationally efficient while solving stiff reaction kinetics. Overall, the proposed 1D model is efficient and also physically more complete owing to the inclusion of a particle model. Hence, the proposed 1D particle-reactor model can help to design and operationalize all kinds of gas-solid packed bed reactions.

ACKNOWLEDGMENT

The work has been carried out as a part of a POP-SEP funding from SINTEF Materials and Chemistry and funding from the European Union Seventh Framework Programme (FP7/2007–2013) under grant agreement n° 268112 (Project acronym DEMOCLOCK).

REFERENCES

[1] G. Eigenberger, Catalytic Fixed-Bed Reactors. Handbook of Heterogeneous Catalysis. , 2008, p. 2075.
[2] J.B. Joshi, L.K. Doraiswamy, Chemical Reaction Engineering, in Albright's Chemical Engineering Handbook, CRC Press. Albright, Boca , Raton, FL, 2009, p.
[3] S. Noorman, Packed bed reactor technology for chemical-looping combustion, Univ.**2009**.p.
[4] S. Noorman, F. Gallucci, M. Van Sint Annaland, J.A.M. Kuipers, *Industrial and Engineering Chemistry Research* **2011**, *50*, 1968.
[5] K.R. Rout, H.A. Jakobsen, *Fuel Processing Technology* **2013**, *106*, 231.
[6] K.R. Rout, J. Solsvik, A.K. Nayak, H.A. Jakobsen, *Chem Eng Sci* **2011**, *66*, 4111.
[7] S. Noorman, F. Gallucci, M. Van Sint Annaland, J.A.M. Kuipers, *Chemical Engineering Journal* **2011**, *167*, 297.
[8] S. Noorman, F. Gallucci, M.M. van Sint Annaland, J.A.M. Kuipers, *Chemical Engineering Journal* **2011**, *167*, 369.
[9] G.D. Ingram, I.T. Cameron, K.M. Hangos, *Chem Eng Sci* **2004**, *59*, 2171.
[10] S. Ergun, *Chem. Eng. Prog* **1952**, *48*, 89.
[11] W.E. Ranz, W.R. Marshall, *Chem. Eng. Prog.* **1952**, *48*, 173.
[12] M.V. Tabib , S.T. Johansen , A. Shahriar, *Industrial and Engineering Chemistry Research* **2013**, *52 (34)* 12041.
[13] A.C. Hindmarsh, R.S. Stepleman, "ODEPACK, a Systematized Collection of ODE Solvers" Scientific Computing, RR. S. Stepleman et al., eds., North-Holland, Amsterdam, 1983, p. 55.
[14] G.D. Byrne, A.C. Hindmarsh, *ACM Trans. Math. Software* **1975**, *1*, 71.
[15] P.N. Brown, G.D. Byrne, A.C. Hindmarsh, *SIAM J. Sci. Stat. Comput.* **1989**, *10*, 1038.
[16] J.E. Crider, A.S. Foss, *AIChE J.* **1968**, *14*, 77.
[17] S.V. Patankar, Numerical heat transfer and fluid flow / Suhas V. Patankar, Hemisphere Pub. Corp. ; McGraw-Hill, Washington : New York, **1980**.p.
[18] V. Spallina, F. Gallucci, M.C. Romano, P. Chiesa, G. Lozza, M. van Sint Annaland, *Chemical Engineering Journal* **2013**, *225*, 174.
[19] B.P. Leonard, S. Mokhtari, ULTRA-SHARP Nonoscillatory Convection Schemes for High-Speed Steady Multidimensional Flow, NASA TM 1-2568 (ICOMP-90-12)NASA Lewis Research Center, 1990, p.